

1 Chromosome-scale *Salvia hispanica* L. (Chia) genome assembly reveals rampant *Salvia*
2 interspecies introgression

3 Julia Brose¹, John P. Hamilton^{2,3}, Nicholas Schlecht⁴, Dongyan Zhao¹, Paulina M. Mejía-Ponce⁵,
4 Arely Cruz Pérez⁵, Brieanne Vaillancourt², Joshua C. Wood², Patrick P. Edger⁶, Salvador Montes-
5 Hernandez⁷, Guillermo Orozco de Rosas⁸, Björn Hamberger⁴, Angélica Cibrian Jaramillo⁵, and C.
6 Robin Buell^{2,3,9}

7 ¹Department of Plant Biology, Michigan State University, East Lansing, MI, USA

8 ²Center for Applied Genetic Technologies, University of Georgia, Athens, GA, USA

9 ³Department of Crop and Soil Sciences, University of Georgia, Athens, GA, USA

10 ⁴Department of Biochemistry and Molecular Biology, Michigan State University, East Lansing,
11 MI, USA

12 ⁵National Laboratory for Genomics of Biodiversity (UGA-Langebio), CINVESTAV, Irapuato,
13 Guanajuato, Mexico

14 ⁶Department of Horticulture, Michigan State University, East Lansing, MI, USA

15 ⁷Campo Experimental Bajío, Instituto Nacional de Investigaciones Forestales, Agrícolas y
16 Pecuarias, Km 6.5 carretera Celaya-San Miguel de Allende, C.P. 38110, Celaya, Guanajuato,
17 México.

18 ⁸CHIABLANCA SC DE RL, Acatic, Jalisco. Mexico

19 ⁹Institute of Plant Breeding, Genetics, and Genomics, University of Georgia, Athens, GA, USA

20

21

22

23

24 ABSTRACT

25 *Salvia hispanica* L. (Chia), a member of the Lamiaceae, is an economically important crop in
26 Mesoamerica, with health benefits associated with its seed fatty acid composition. Chia
27 varieties are distinguished based on seed color including mixed white and black (Chia pinta) and
28 black (Chia negra). To facilitate research on Chia and expand on comparative analyses within
29 the Lamiaceae, we generated a chromosome-scale assembly of a Chia pinta accession and
30 performed comparative genome analyses with a previously published Chia negra genome
31 assembly. The Chia pinta and negra genome sequences were highly similar as shown by a
32 limited number of single nucleotide polymorphisms and extensive shared orthologous gene
33 membership. There is an enrichment of terpene synthases in the Chia pinta genome relative to
34 the Chia negra genome. We sequenced and analyzed the genomes of 20 Chia accessions with
35 differing seed color and geographic origin revealing population structure within *S. hispanica* and
36 interspecific introgressions of *Salvia* species. As the genus *Salvia* is polyphyletic, its evolutionary
37 history remains unclear. Using large-scale synteny analysis within the Lamiaceae and
38 orthologous group membership, we resolved the phylogeny of *Salvia* species. This study and its
39 collective resources further our understanding of genomic diversity in this food crop and the
40 extent of inter-species hybridizations in *Salvia*.

41 PLAIN LANGUAGE SUMMARY

42 Chia pinta is an economically important crop due to the high fatty acid present in the seeds.
43 There are multiple types of Chia based on the seeds color including mixed which and black (Chia
44 pinta), black (Chia negra), and white (Chia blanca). We generated a genome assembly of Chia
45 pinta and compared it to existing genome assemblies. While the assemblies are highly similar
46 there are key differences in terpene synthase composition between Chia pinta and Chia negra.
47 We also sequenced 20 other Chia accessions with different seed color and geographic origin to
48 determine a population structure within Chia. We generated genomic resources to further our
49 understanding of this food crop.

50 ABBREVIATIONS

51 BGC Biosynthetic gene cluster
52 BUSCO Benchmarking Universal Single Copy Orthologs
53 GO Gene ontology
54 SNP Single nucleotide polymorphism
55 TIR Terminal inverted repeat

56 TPS Terpene synthase

57 WGS Whole genome shotgun

58

59

60 **INTRODUCTION**

61 Chia (*Salvia hispanica* L.) belongs to the largest genus within the Lamiaceae containing
62 approximately 980 species (Hu et al., 2018). Chia is a notable and economically important
63 species within the *Salvia* genus attributable to the high nutritional value of its seeds which
64 contain 16-26% protein, 23-41% fiber, and 20-34% polyunsaturated fatty acids, of which, 60% is
65 α -lineolic acid (Muñoz et al., 2013). Historically, Chia was the third most economically
66 important crop in Mesoamerica, only behind maize and amaranth, due to its use in religious
67 practices and as a medicine (Valdivia-López & Tecante, 2015). The medicinal properties of Chia
68 include treatments for gastrointestinal, respiratory, urinary, obstetrics, skin, central nervous,
69 and ophthalmologic issues (Cahill, 2003). The traditional uses of Chia revolve around religious
70 practices which contributed to the decrease of Chia prominence and cultivation in the 15th
71 century following the invasion by conquistadors (Cahill, 2003). Chia was introduced to Spain
72 where it was named by Linnaeus as *Salvia hispanica* referencing the presumed origin of Spain
73 (Baldivia, 2018). While Chia originated in present day Mexico and Guatemala, it has since been
74 distributed throughout the world resulting in the emergence of diverse varieties (Cahill, 2004).

75 Chia varieties are characterized by their seed color and origin. The widely cultivated Chia
76 blanca has a white seed coat while Chia negra has a black seed coat that can occur in wild and
77 cultivated populations. Other seed coat colors include mixes of black and white seeds.
78 Morphological characteristics distinguishing cultivated from wild accessions mirror traits
79 observed in other domesticated species, such as decreased apical dominance, increased
80 branching, increased seed size, decreased pubescence, increased florescence length
81 determinism, increased anthocyanin pigmentation, variation in seed coat color and patterns,
82 increased plant height, and closed calyxes (Cahill, 2004). While phenotypically distinct, dietary
83 proteins are similar in wild and cultivated Chia accessions although wild accessions with higher
84 levels of polyunsaturated fatty acids have been reported (Peláez et al., 2019).

85 Robust genomic resources for the Lamiaceae facilitate comparative genomic analysis.
86 Within the Lamiaceae there are seven subfamilies with chromosome-scale genomes
87 [Ajugoideae, Callicarpoideae, Nepetoideae, Lamiodeae, Scutellariodeae, and Tectonoideae]
88 (Dong et al., 2018; Zhao et al., 2019a; b; Hamilton et al., 2020; He et al., 2022; Li et al., 2022;
89 Shen et al., 2022; Sun et al., 2022; Pan et al., 2023). Current genomic resources for Chia include
90 a genome assembly derived from an Australian black seeded variety (Chia negra; Wang et al.,
91 2022), a white seeded variety (Chia blanca; Li et al., 2023), and a Mexican Chia (Alejo-Jacuinde
92 et al., 2023) as well as transcriptomes constructed from wild and cultivated seeds (Peláez et al.,
93 2019). Expanding the number and diversity of chia accessions with genome assemblies and
94 sequence will facilitate our understanding of genetic diversity of this important crop as well as

95 provide resources for more informed breeding programs. In addition to diversity within Chia,
96 three other *Salvia* species occur in the same region in Mesoamerica (*Salvia uruapan* Fern.,
97 *Salvia tiliifolia* Vahl., and *Salvia polystachya* Ort.) that have similar uses as *S. hispanica* (Cahill,
98 2003). These species are challenging to distinguish from each other, but no reports indicate
99 hybridization with *S. hispanica*. A phylogeny of *Salvia*, based on 91 nuclear genes, places Chia
100 within *Salvia* sect. *Potiles* in a monophyletic clade (Lara-Cabrera et al., 2021). However, the
101 *Salvia* genus has yet to be fully resolved and remains polyphyletic with *S. tiliifolia* being placed
102 within two separate clades: the Angulatae and Polystachyae (Lara-Cabrera et al., 2021).
103 Therefore, additional phylogenetic analyses are necessary to achieve a comprehensive
104 resolution of the *Salvia* genus.

105 In this study, we report on the genome sequence of a Chia pinta accession, comparative
106 analyses with published Chia genomes, and analysis of genetic diversity in a set of 20 Chia
107 accessions revealing population structure between domesticated and wild Chia species and
108 evidence of interspecies hybridization of *S. tiliifolia* with Chia.

109 RESULTS AND DISCUSSION

110 Chia Genome

111 We selected a Chia pinta accession from Acatic, Jalisco, Mexico that produces mixed
112 color seeds and is grown as a superfood source throughout Mexico. Using 5.7 million PacBio
113 long reads (36.5 Gb) representing ~100x coverage of the predicted ~355 Mbp Chia genome
114 (Wang et al., 2022), we assembled the Chia pinta (2n=2x=12) genome using Canu (Koren et al.,
115 2017). Whole genome shotgun (WGS) reads were used to generate a k-mer (k=21) distribution
116 profile using GenomeScope indicating an estimated genome size of 338 Mbp with 62.6% unique
117 kmers and 0.5% heterozygosity. The initial Canu assembly was error corrected using the raw
118 PacBio reads using Arrow (Pacific Biosciences) followed by three rounds of error correction with
119 the Illumina WGS reads using Pilon (Walker et al., 2014). The error-corrected assembly
120 consisted of 2,094 contigs with a total length of 425.14 Mbp, which is substantially larger than
121 the previously estimated genome size. Haplontigs were removed from the assembly using
122 purgeHaplontigs (Roach et al., 2018) (-a = 50%) with an output consisting of “primary contigs”
123 representing the putative haploid genome sequence, “haplontigs” containing diverged
124 haplotypes, and “artefacts” representing contigs with very low or extremely high read
125 coverage. Following removal of haplontigs, the “primary contigs” size decreased from 425 Mbp
126 to 343 Mbp (Table 1). Manual examination of Chia vs. Chia self-alignments of contigs in the
127 ‘purged assembly’ revealed five pairs of contigs that were putative residual haplontigs. Removal
128 of these contigs resulted in a ‘purged assembly’ containing 407 contigs with an N50 contig
129 length of 1.5 Mbp and a total size of 343.2 Mbp. The distribution of k-mers from WGS reads in

130 the final assembly was examined using KAT (Mapleson et al., 2017) revealing a single peak
131 indicating a haploid assembly with few retained haplotigs.

132 Using Hi-C sequence data, the contigs were assembled into six pseudomolecules,
133 consistent with the known chromosome number of Chia and the Chia negra Australian Black
134 (hereafter Chia negra) genome assembly (Wang et al., 2022). The final Chia pinta genome
135 assembly was 342 Mb final with an N50 of 62Mb, of which, 99.64% of the assembly was
136 anchored to one of the six pseudochromosomes (Table 1). Metrics for the final chromosome
137 assembly were calculated using only the six chromosomes. The GC content of the final assembly
138 was 36.6% consistent with the previously published Chia negra genome (Wang et al., 2022).
139 Alignment of Illumina WGS reads to the final assembly revealed 98.4% of the reads aligned to
140 the genome, of which, 99.5% were properly paired. Alignment of RNA-seq reads from a diverse
141 set of tissue types (leaf, inflorescence, stem, and root) showed an overall alignment rate
142 between 93.7% and 96.0%. To confirm the quality of the Chia pinta assembly, we used
143 Benchmarking Universal Single Copy Orthologs (BUSCO) (Simão et al., 2015) to determine the
144 representation of conserved orthologs in the final assembly. In total, 97.4% of the BUSCO
145 orthologs were complete with 86.6% as single copy, 10.8% duplicated, 0.7% fragmented, and
146 1.9% missing. Overall, these results indicate a high-quality Chia pinta genome assembly.

147 **Repetitive Sequences and Transposable Element Annotation in the Chia pinta genome**

148 Using *de novo* repetitive sequence identification with RepeatModeler coupled with sequences
149 from the Viridiplantae RepBase, RepeatMasker masked 46.8% of the Chia pinta genome. With
150 respect to transposable elements, retroelements were the dominant sequence with 40,151
151 retroelements occupying 15.15% of the Chia pinta genome while DNA transposons (36,807
152 elements) accounted for 4.86%. Unclassified interspersed repeats represented the largest
153 number of elements with 378,795 or 26.11% of the genome. The remaining repetitive elements
154 included rolling circle, small RNA, satellites, simple repeats, and low complexity sequences
155 make up less than 1% of the genome.

156 The Extensive *de-novo* TE Annotator (EDTA) was used to annotate the Chia pinta
157 genome for transposable elements revealing 314,306 elements spanning 149,780,410 bp
158 (43.64%) of the Chia pinta genome. Long terminal repeats comprise 21.33% of the genome, of
159 which, 5.7% were *Copia* elements and 11.45% were *Gypsy* elements; unknown long terminal
160 repeats comprise 4.13% of the genome. Terminal inverted repeat (TIR) sequences represent
161 20.01% of the genome with the largest portion (12.09%) belonging to Tc1_Mariner family. The
162 remaining TIRs are PIF_Harbinger (3.26%), hAT (2.32%), Mutator (1.80%), and CACTA (0.54%).
163 Helitrons are non-terminal inverted repetitive elements and comprise 2.3% of the genome.

164

165 **Annotation of the Chia Pinta Genome**

166 We annotated the Chia pinta genome for protein-coding genes resulting in 59,062
167 working gene models corresponding to 41,279 loci (Table 2). Working gene models had an
168 average transcript length of 3.1 kbp, coding sequence (CDS) length of 1,217 bp, exon length of
169 279 bp and intron length of 240 bp. Working gene models exhibited an average of 5.8 exons,
170 with 13.6% of transcripts being single-exon genes. The high confidence model set, a subset of
171 the working set which have expression and/or protein evidence, contains 53,053 gene models
172 representing 35,480 loci (Table 2). The high confidence set has an average transcript length of
173 3.3 kbp, exon length of 226 bp, intron length of 244 bp, and 6.1 exons per model; 6,105 gene
174 models are single exon models. We selected the longest model as a representative for each
175 gene locus from the working and high confidence model sets. With respect to BUSCO
176 representation, the high confidence representative models are 94.8% complete, of which,
177 84.8% are complete and single copy while 10% are complete and duplicated; 1.9% are
178 fragmented and 3.3% are missing. For the working representative models, 95.7% are complete
179 with 85.5% complete and single copy and 10.2% complete and duplicated; 1.7% fragmented
180 and 2.6% missing. Overall, the BUSCO results indicate a robust annotation of the Chia pinta
181 genome.

182 **Comparative Analyses of Chia Genome Assemblies**

183 There are currently three published long-read, chromosome-scale Chia genome
184 assemblies: Chia blanca (Li et al., 2023), Chia negra (Wang et al., 2022), and Mexican Chia
185 (Alejo-Jacuinde et al., 2023). BUSCO analysis of all three published Chia genomes revealed that
186 all of these assemblies were high quality and with robust gene annotation datasets. Syntenic
187 orthologs (syntelogs) were identified between all four assemblies revealing a high degree of
188 synteny between these genome assemblies (Figure 1) with limited disruptions that may be due
189 to assembly artifacts in the various genome assemblies. Due to the high degree of similarity
190 between the four Chia genomes, we performed detailed comparisons of our Chia pinta genome
191 to the chromosome-scale black seeded Chia negra in which 73.62% of the genes were colinear
192 within 1,178 syntetic blocks (Figure 1). Chia negra is a 344Mb genome assembly with 99.05%
193 anchored on to chromosomes and 3.3Mb unanchored (Wang et al., 2022) with 428 gaps,
194 amounting to a total of 191.2 kbp Ns. A total of 1,278,367 Single Nucleotide Polymorphisms
195 (SNPs) were identified between the Chia negra and Chia pinta genomes that were distributed
196 throughout the genome with 10.0% (127,210) residing in genic regions, 75.6% (967,385) in
197 intergenic regions, and 14.4% (184,772) within intronic regions of the Chia pinta genome.

198 Using Orthofinder with the predicted proteomes of both Chia pinta and Chia negra, we
199 identified 20,580 orthogroups, of which, 358 orthogroups (2,738 genes) were unique to Chia
200 pinta while 462 orthogroups (1,458 genes) were unique to Chia negra. Gene ontology (GO)

201 enrichment of the genes unique to Chia pinta revealed differences in certain biological process,
202 cellular components, and molecular function ontologies. Of particular interest was the
203 enrichment of the GO terms “defense response”, and “diterpenoid biosynthetic process” with
204 45 terpene synthases identified in the GO terms “diterpenoid biosynthetic process” and
205 “terpene synthase activity”.

206 BLASTP was used to search all representative proteins in Chia pinta and Chia negra
207 against a collection of known terpene synthases (TPSs). TPSs greater than 350 amino acids were
208 used to create a phylogeny to determine the relationships among the TPSs. After filtering, a
209 total of 111 TPSs in Chia pinta and 53 in Chia negra were identified. To confirm that this is not
210 due to annotation errors, Chia pinta TPS transcript sequences were used in a BLASTN search
211 against the Chia negra genome; no additional terpene synthases were identified in Chia negra
212 indicating these sequences are absent in the Chia negra genome assembly. A phylogeny was
213 constructed with putative TPS protein sequences from Chia pinta, Chia negra, and functionally
214 characterized TPSs to assign Chia TPSs to closest known functionally characterized TPSs. Despite
215 GO enrichment annotation of ‘diterpenoid biosynthetic process’, most enriched TPSs are within
216 the TPS-a and to a lesser degree TPS-b subfamilies which produce sesqui- and monoterpenes,
217 indicating an expansion of volatile terpenes. The discrepancy on the GO terms claiming
218 diterpenoid processes yet finding sesqui- and monoterpane synthases can be explained by GO
219 enrichment often misannotated TPSs as diTPSs.

220 The TPS-a subfamily contains 56 putative TPSs in Chia pinta and only four in Chia negra.
221 Of the 56 putative Chia pinta TPSs, 38 were found to enriched relative to Chia negra. The
222 enriched TPSs reside in clades that do not contain a Chia negra TPS. To further understand the
223 genomic context of the enriched TPSs, biosynthetic gene clusters (BGCs) membership and
224 synteny were used. There are 16 BGCs containing TPSs in Chia pinta present on chromosomes
225 1, 2, 3, 4, and 6. Notably, six of these BGCs contain 23 out of the 56 Chia pinta specific TPS-a
226 subfamily genes (Figure 2). This coincides with the expansion of the TPS-a subfamily in Chia
227 pinta. All Chia pinta enriched TPS-a BGCs contain syntenic genes between Chia pinta, Chia
228 negra, and *S. miltiorrhiza* (Figure 2). However, Chia pinta only shares one syntenic TPS with Chia
229 negra and three syntenic TPSs with *S. miltiorrhiza*. Many of the TPSs present in Chia pinta’s
230 BGCs appear to be tandem duplications, most notably in the teal and green BGCs (Figure 2).
231 However, some of the TPSs present in the green BGC are less than 350 amino acids indicating
232 they may be truncated.

233 The origin and expansions of TPS-a genes were examined through synteny with *S.*
234 *miltiorrhiza*. Two separate BGCs, purple and orange, contain paralogous TPSs yet are in distinct
235 syntenic blocks (Figure 2). Work in *S. miltiorrhiza* characterized orthologs of these genes (89%
236 identity) as (-)-5-epi-eremophilene synthases in which three TPSs (*SmSTPS1*, *SmSTPS2*, and

237 *SmSTPS3*) had differential gene expression yet identical biochemical activity (Fang et al., 2017).
238 The purple BGC contains one TPS that is a syntelog of *SmSTPS1*, but there are no syntelogs of
239 *SmSTPS2* or *SmSTPS3* (Figure 2) suggesting that a single gene was maintained and was tandemly
240 duplicated or that structural rearrangements occurred disrupting synteny with *SmSTPS2* or
241 *SmSTPS3*. The orange BGC contains TPSs that are equally related to *SmSTPS1* but are not
242 syntenic with the *S. miltiorrhiza* *SmSTPS* cluster. Instead, the homologs have moved into a
243 different syntenic block entirely. Additionally, there is a notable difference in gene expression
244 profiles of the purple and orange BGCs with the orange BGC largely expressed in the leaf and
245 stem whereas the purple clade has its highest expression in roots amongst the different
246 paralogs (Figure 2). This may exemplify how a BGC can evolve by duplication and
247 subfunctionalization resulting in distinct spatial gene expression patterns. The teal and yellow
248 BGCs indicate that there are no syntenic TPSs in *S. miltiorrhiza*. The minor enrichment in TPS-b
249 genes present in Chia pinta is largely due to expansion of a single clade. The closest functionally
250 characterized enzyme to this expanded clade was and (–)-exo- α -bergamotene synthase, having
251 between 62–67% identity for this clade.

252 Finding such a large difference in TPS-a abundance and identifying many of them within
253 BGCs between Chia pinta and Chia negra further supports the diversity that exists not just
254 within the *Salvia* genus, but even within Chia accessions. One potential source of the TPS
255 expansion could be due to sequencing gaps in the Chia negra genome assembly. Specially, there
256 are gaps in the purple BGC region of the Chia negra genome sequence. Therefore, these TPSs
257 could be present within the species, but were not captured by the genome assembly. However,
258 for the remaining five BGCs there are no assembly gaps in the Chia negra genome assembly and
259 when the predicted transcripts for the TPSs were searched against the Chia negra genome,
260 there were no hits for these regions. To determine if the TPSs are unique to Chia pinta, we
261 examined the BGCs for syntelogs in the two other long-read Chia genome assemblies. The teal,
262 orange, pink, green, and yellow BGCs contain syntelogs in Chia pinta, Chia blanca, and Mexican
263 Chia whereas the purple BGC contains only syntelogs between Chia pinta and Mexican Chia.
264 Thus, diversity in TPSs is present between Chia accessions suggesting variation in terpenoid
265 profiles that may be associated with local adaptation.

266 **Lamiaceae Phylogeny and Gene Family Expansions**

267 To determine the evolutionary relationships of Lamiaceae species with Chia pinta, a
268 species phylogeny was constructed using high-quality available genome sequences from 23
269 species from seven tribes in the Lamiaceae (Figure 3). Using the multiple sequence alignment
270 option in Orthofinder, 923,746 genes were assigned to orthogroups. As shown in Figure 3, the
271 Nepetoideae tribe is sister to Ajugoideae, Lamiodeae, and Scutellariodeae, the Callicarpoideae
272 and Tectonoideae are sister to all other species, and the Premnoideae is sister to all other

273 subfamilies. The relationships between the tribes in this genome-derived tree differs from a
274 published phylogeny derived from 520 single copy transcripts (Godden et al., 2019) in which the
275 Nepetoideae is sister to Ajugoideae, Lamiodeae, Scutellariodeae, Premnoideae, and
276 Tectonoideae. The topology difference between these two phylogenetic estimates could be due
277 to a combination of species sampling and data quality differences.

278 Gene expansions and contractions of single copy orthologs throughout the Lamiaceae
279 were identified using CAFE (Figure 3A) and placed on the species tree phylogeny revealing large
280 expansions and contractions throughout the Lamiaceae. The node branching of the
281 Nepetoideae indicates a gene family expansion of 1,506 genes and contraction of 1,688 genes.
282 The branch point from *S. hispanica* and *Salvia splendens* reveals 2,901 gene expansions and
283 12,295 gene contractions indicating substantial differences within the *Salvia* genus.

284 Synteny between genomes serve as a tool for examining evolution reflecting ancestral
285 conservation of gene order. Using Chia pinta as the reference genome, we examined synteny
286 within 11 chromosome-scale assemblies, spanning six tribes of the Lamiaceae family, revealing
287 extensive conservation among the genomes (Figure 3B). In total, 182 Chia pinta genes were
288 found to have a one-to-one syntenic relationship across all 11 species.

289 The polyphyletic nature of *Salvia* is highlighted by orthogroup membership. Of the
290 39,379 orthogroups containing 211,888 genes there were 12,987 orthogroups, containing
291 165,520 genes, in common among all *Salvia* (Figure 4A). The next highest number of
292 orthogroups are unique to *S. rosmarinus* closely followed by *S. officinalis* and then *S. splendens*
293 (Figure 4A). We also performed syntenic analyses between the genomes of four *Salvia* species
294 to further our understanding of the species relationship in this polyphyletic genus. As expected,
295 Chia pinta shares extensive synteny with other *Salvia* species (Figure 4b). *S. splendens* is
296 reported to be a tetraploid (Jia et al., 2021). Based on orthogroup membership, 25% (4,684) of
297 orthogroups shared by *S. splendens* and Chia pinta contain two *S. splendens* genes for each Chia
298 pinta gene. This pattern reflects that *S. splendens* is a tetraploid and Chia pinta is a diploid.
299 There are also two syntenic blocks in *S. splendens* for each block within Chia pinta, the syntenic
300 blocks exist across four chromosomes in *S. splendens* (Figure 4b and 4c). It has been reported
301 that there is a single shared whole genome duplication between Chia pinta and *S. splendens*
302 and an additional duplication just in *S. splendens* (Jia et al., 2021; Wang et al., 2022). Therefore,
303 the four unique chromosomes syntetic to a single chromosome in Chia pinta could be due to
304 chromosomal fusions in Chia pinta or chromosomal fissions in *S. splendens*. Within the *Salvia*
305 genus there are large regions of fragmented synteny between Chia pinta and *S. officinalis* as
306 well as between *S. splendens* and *S. officinalis*. The fragmentation could be present due to
307 different ancestry of Chia pinta and *S. officinalis*. As *Salvia* is a polyphyletic genus (Lara-Cabrera
308 et al., 2021), this could be indicative of how distantly related these two species are. An

309 alternative hypothesis is that they share a common ancestor, but the divergence time between
310 species is so long that conserved genetic regions have been differentially fractionated (i.e.
311 unique gene loss patterns). This is consistent with the large gene family expansions and
312 contractions in the node that splits the *Salvia* species.

313 **Population Structure of Chia**

314 Seed coat color is a frequent descriptor for Chia accessions with Chia white seeded
315 blanca varieties while Chia negra, Chia cualac, and Chia xonostli are predominately black-
316 seeded (Figure 5a). Chia pinta seeds are a mix of both black and white seeds (Figure 5a). A
317 diversity panel of 19 Chia accessions including wild and cultivated accessions along with two *S.*
318 *tiliifolia* accessions with origins throughout Mexico was constructed and sequenced to reveal
319 genetic diversity among accessions and provide insight into population structure of cultivated
320 and wild Chia varieties. The percentage of reads aligned to the Chia pinta genome ranged from
321 95.5% to 97.7% for the *S. tiliifolia* samples and 96.3%-98.5% for the Chia varieties suggesting
322 that the two species share substantial sequence similarity. Population structures were inferred
323 with admixture with $k=2$ to $k=13$. Population structure admixture results suggested through
324 the cross-validation error plot that there are two possible number of populations: four and nine
325 as the local minima being at four and the global minima at nine in the cross-validation error
326 plot.

327 Using a $k=4$, broad population groups are present that can be assigned to known
328 categories of Chia: Chia pinta (yellow), *S. tiliifolia* (purple), Chia negra and Chia Xonostli (blue),
329 and Chia Cualac (pink). The population structure indicates that the phenotypic and origin
330 grouping reflects the genetic structure of the population. Chia pinta accessions are
331 domesticated Chia varieties whereas Chia negra and Chia Xonostli are classified as wild due to
332 their more open calyx and other wild traits. Chia negra is in the same population group with the
333 less widely known Chia Xonostli which is similar to Chia negra yet categorized differently due to
334 its domesticated traits. Historically, Chia Xonostli was found in the states of Jalisco, Guanajuato,
335 Veracruz, and Hidalgo. Chia Cualac was reported to be semi-domesticated and forms their own
336 group with some admixture from Chia Xonostli (Peláez et al., 2019). This follows the hypothesis
337 that wild introgressions are present throughout the populations. One *S. tiliifolia* accession is
338 admixed with Chia pinta. *S. tiliifolia* is nearly indistinguishable from Chia and is known to grow
339 in the same areas as Chia pinta; thus, it is possible that these species hybridize and form a
340 population of *S. tiliifolia* that is highly admixed with Chia pinta. Feral hybrid accessions could
341 continue to evolve through hybridization with domesticated Chia yielding the admixture
342 present within one accession of *S. tiliifolia* (Figure 5).

343

344 CONCLUSIONS

345 In this study, a high-quality chromosome-scale genome assembly of Chia pinta was generated
346 that allowed for additional genomic comparisons within the economically important crop
347 including three other long-read, chromosome-scale Chia assemblies that showed extensive
348 synteny among the genome sequences. Comparative genomic tools were used to determine
349 differences within Chia accessions and throughout the Lamiaceae. Interestingly, Chia pinta was
350 enriched in TPSs and contains novel TPSs compared to the Chia negra with some TPSs located
351 within BGCs and syntenic with *S. miltiorrhiza*. Further examination of TPSs within BGCs among
352 the four Chia genome assemblies revealed further diversification suggestive of variation in
353 terpenoid biosynthesis among varieties. Through sequencing of a diversity panel, the
354 population structure of Chia revealed introgression with other *Salvia* species.

355 MATERIALS AND METHODS

356 Plant materials

357 Different Chia varieties were collected throughout Mexico. Plants were grown in an
358 experimental field in Celaya, Guanajuato, Mexico (20.578°, -100.822°) at the Instituto Nacional
359 de Investigaciones Forestales, Agrícolas y Pecuarias (INIFAP).

360 Nucleic acid isolation, library construction, and sequencing

361 For construction of a reference genome, DNA was isolated from medium-sized leaves from a
362 mature plant (13.5 weeks old) of accession SM_ACJ2017 using a modified protocol from Doyle
363 and Doyle (1987) and Healey *et al.* (2014). Large insert (>15kb, >20kb) PacBio libraries were
364 made with the SMRTbell™ Template Prep Kit and sequenced on the PacBio Sequel platform at
365 the University of Georgia, Georgia Genomics and Bioinformatics Core (GGBC, UG Athens, GA,
366 RRID:SCR_010994). A whole genome shotgun library for reference error correction was
367 prepared using the Illumina TruSeq Nano DNA Library Preparation Kit and sequenced in paired-
368 end mode, 150 nt in length on a HiSeq 4000 at the Michigan State University Research
369 Technology Support Facility (RTSF). Whole genome shotgun libraries for use in error correction
370 and diversity panel variant analyses were constructed as described previously in Hardigan *et al.*
371 2016 (Hardigan *et al.*, 2016) and sequenced at the Michigan State University RTSF in paired-end
372 mode on a HiSeq4000 generating 150 nt reads. RNA was isolated from three biological
373 replicates from a core set of tissues (leaf, inflorescence, lateral stem, secondary root) from the
374 reference accession SM_ACJ2017 as described previously in Peláez *et al.* 2019 (Peláez *et al.*,
375 2019). RNA-seq libraries were prepared using the Illumina TruSeq Stranded mRNA Library
376 Preparation Kit and sequenced on an Illumina HiSeq 4000 generating 150 nt paired end reads
377 for one replicate and 50 nt single end reads for the other two replicates; library preparation and
378 sequencing were performed at the Michigan State University Research Technology Support

379 Facility (RTSF). A Phase Genomics Proximo Hi-C library was prepared from Chia pinta leaf tissue
380 and sequenced by Phase Genomics (Seattle, WA) on the NextSeq 500 generating paired end
381 150 nt reads.

382 **Chia pinta genome assembly**

383 PacBio reads greater than 10 kbp (1.2 million reads, 21.6 Gb) were used to generate the initial
384 assembly using Canu (v1.7; Koren et al., 2017) with a corrected ErrorRate of 0.15%. The initial
385 assembly was polished with the raw PacBio reads using Arrow in the SMRT Analysis package
386 (v5.0.1.9585; Pacific Biosciences), followed by three rounds of error correction with 56 million
387 Illumina WGS reads (150 nt paired-end WGS reads, 45X coverage) using Pilon (v1.22; Walker et
388 al., 2014). Potential haplotigs were purged using purgeHaplots (v1.0.4; Roach et al., 2018)
389 with the “maximum match score (-m)” of 500% and “-a = 50%”. Contigs were scaffolded to a
390 chromosome scale assembly using Hi-C reads and Proximo pipeline with an input chromosome
391 number of six by Phase Genomics (Bickhart et al., 2017). Scaffolded contigs were visualized with
392 Juicebox (v1.9.8; Durand et al., 2016).

393 **Genome annotation**

394 A custom repeat library (CRL) was generated using RepeatModeler (v2.0.1; Flynn et al.,
395 2020) and protein coding genes were removed from the CRL using ProteinExcluder (v1.2;
396 Campbell et al., 2014). The Viridiplantae RepBase repeats (v20150807) were then added to
397 create the final CRL. The genome assembly was hard and soft masked using RepeatMasker
398 (v4.1.0; Smit et al.) with the CRL with the parameters: -s -nolow -no_is. RNA-seq libraries were
399 cleaned using Cutadapt (v2.9; Martin, 2011) (--times 2 --minimum-length 100 --quality-cutoff
400 10) and then aligned to the genome assembly with HISAT2 (v2.2.0; Kim et al., 2019) (--max-
401 intronlen 5000 --rna-strandness RF -dta -no-unal). The RNA-seq alignments were then
402 assembled into transcript assemblies using Stringtie (v2.1.1; Kovaka et al., 2019).

403 *Ab initio* gene models were predicted on the soft-masked genome assembly using the
404 BRAKER2 pipeline (v2.1.5; Brůna et al., 2021) using the leaf RNA-seq library CHI_AA as a source
405 for hints. The *ab initio* gene models were then refined using PASA2 (v2.4.1; Campbell et al.,
406 2006) with the RNA-seq transcript assemblies as a source of transcript evidence to produce the
407 working gene model set. High confidence gene models were selected from the working gene
408 model set by first calculating working gene model abundances of the RNA-seq libraries for the
409 working gene models with Kallisto (v0.46.0; Bray et al., 2016), then searching the working gene
410 models against PFAM (v32.0; Mistry et al., 2021) with HMMER (v3.2.1; Mistry et al., 2013).
411 Working gene models with a TPM >1 in at least one RNA-seq library or a non-transposable
412 element related PFAM domain match and no partial or containing an internal stop codon were
413 identified as high confidence gene models. Functional annotation was assigned to the working

414 gene model by searching the protein sequences against the *Arabidopsis* proteome (TAIR10),
415 PFAM (v32.0; Mistry et al., 2021) and the Swiss-Prot plant proteins (release 2015_08). Search
416 results were processed in the same order and the function of the first hit encountered was
417 assigned to the gene model. Repetitive elements were identified using EDTA (v2.1.0; Ou et al.,
418 2019) with the parameters species set to “others” and step set to “all”.

419 **Genome quality assessment**

420 Quality assessment of the genome assembly was performed by aligning WGS reads cleaned for
421 low quality bases and adaptors using Cutadapt (v3.4; Martin, 2011) to the final assembly using
422 BWA-mem (v0.7.16a; Li, 2013). Assemblathon.pl
(https://github.com/KorfLab/Assemblathon/blob/master/assemblathon_stats.pl) was used to
423 generate genome metrics. BUSCO (v3.1.0.Py3; Simão et al., 2015) *embryophyta_odb10* was
424 used to determine genic representation in the final assembly. Jellyfish (v.2.3.0; Marçais &
425 Kingsford, 2011) with the option -m 21 was used to count kmers that were then visualized in
426 GenomeScope (v2.0; Ranallo-Benavidez et al., 2020) with kmer length 21 was used to verify
427 genome size and heterozygosity from the WGS reads from Chia pinta (CHI_AN). The Kmer
428 Analysis Toolkit (v2.4.1; Mapleson et al., 2017) was used to examine the assembly for retained
429 haplotigs. Synteny between the chia genome assemblies (Wang et al., 2022; Alejo-Jacuinde et
430 al., 2023; Li et al., 2023) was analyzed using GENESPACE (v.1.1.10; Lovell et al., 2022). Syntenic
431 comparison between Chia pinta and Chia negra was also performed using MCScanX (Wang et
432 al., 2012).

434 **Lamiaceae phylogeny and comparative analysis**

435 Publicly available genomes of *Callicarpa americana* (Hamilton et al., 2020), *Cleorodendrum*
436 *inerme* (He et al., 2022), *Hyssopus officinalis* (Lichman et al., 2020), *Nepeta cataria* (Lichman et
437 al., 2020), *Nepeta mussinii* (Lichman et al., 2020), *Ocimum basilicum* (Bornowski et al., 2020),
438 *Origanum majorana* (Bornowski et al., 2020), *Origanum vulgare* (Bornowski et al., 2020), *Perilla*
439 *frustescens* (Zhang et al., 2021; Tamura et al., 2022), *Pogostemon cablin* (Shen et al., 2022),
440 *Salvia miltiorrhiza* (Pan et al., 2023), *Salvia officinalis* (Li et al., 2022), *Salvia rosmarinus*
441 (Bornowski et al., 2020), *Salvia splendens* (Jia et al., 2021), *Scutellaria baicalensis* (Zhao et al.,
442 2019b), *Scutellaria barbata* (Xu et al., 2020), *Tectona grandis* (Zhao et al., 2019a), *Thymus*
443 *quinquecostatus* (Sun et al., 2022), *Lavandula angustifolia* (Hamilton et al., 2023) and *Premna*
444 *obstusifolia* (He et al., 2022) were obtained and quality assessed using BUSCO (v5.5.0; Simão et
445 al., 2015) *embryophyta_odb10*. Species with genome assembly complete BUSCO scores greater
446 than 90% and annotation complete BUSCO scores greater than 80% were used in further
447 comparative analysis. Orthogonal genes and species tree phylogeny were built using
448 OrthoFinder (v.2.5.4; Emms & Kelly, 2019) with options -M msa -T raxml. The species tree
449 output was converted into an ultrametric tree using the make_ultrametric command in

450 OrthoFinder (v.2.5.4; Emms & Kelly, 2019). Branch lengths were rescaled using the *Premna*
451 *obstusifolia* divergence date of 16.06 MYA retrieved from the TimeTree of Life resource (Kumar
452 et al., 2022). Gene family expansions and contractions were identified using CAFE (v.4.2.1; Han
453 et al., 2013) with the following scripts with default parameters: `cafutorial_report_analysis.py`
454 and `cafutorial_draw_tree.py`. Syntelogs through the Lamiaceae were obtained for the
455 chromosome scale assemblies within the Lamiaceae and visualized using GENESPACE (v.1.1.10;
456 Lovell et al., 2022).

457 **Gene ontology term enrichment**

458 Gene ontology (GO) terms were assigned to high confidence Chia pinta genes using
459 InterProScan (v5.63-95.0; Jones et al., 2014). GO descriptions were added using the
460 ontologyIndex package (Greene et al., 2017) and enrichment was calculated using the topGO R
461 package (Alexa & Rahnenfuhrer, 2010). GO terms with an FDR adjusted p-value < 0.05 were
462 considered significant.

463 **Terpene synthase identification**

464 BGCs were identified in Chia pinta, Chia negra, and *S. miltiorrhiza* with PlantSMASH (Kautsar et
465 al., 2017). Enriched TPSs identified in the various BGCs were searched with NCBI BLAST the
466 nonredundant protein database to identify the closest functionally characterized TPSs. To
467 extract all TPSs from the genome, the high confidence representative protein models were
468 blasted against a reference set of known TPSs enzymes representing TPSs across all subfamilies.
469 The BLAST hits with an E-value 1E-5 or better were selected. These gene models were filtered
470 to remove any sequences smaller than 350 amino acids to ensure a quality phylogeny and
471 minimize pseudogenes. The final set of putative and reference TPS sequences were aligned
472 using clustal omega (v1.2.4; Sievers et al., 2011). A phylogenetic tree of the alignment was built
473 via RAXML (v8.2.12; Stamatakis, 2014) with the PROTGAMMA AUTO model, algorithm a, and
474 1000 bootstraps. Gene expression of terpene synthases was calculated using the single end
475 RNA-seq libraries and Cufflinks (v.2.2.1; Roberts et al., 2011) with the options -b and -u to
476 generate FPKM values for all Chia pinta genes. Orthologous genes from Chia pinta, Chia negra
477 (Wang et al., 2022), Chia blanca (Li et al., 2023) and the Mexican Chia variety (Alejo-Jacuinde et
478 al., 2023) were identified using OrthoFinder (v.2.5.4; Emms & Kelly, 2019) with options -M msa -
479 T raxml.

480 **Population structure analysis**

481 Whole genome shotgun reads from the diversity panel were cleaned using Cutadapt (v3.4;
482 Martin, 2011) and aligned to the Chia genome using BWA-mem (v0.7.16a; Li, 2013). PicardTools
483 (v2.20.8; Picard toolkit, 2019) commands SortSam, MarkDuplicates, BuildBamIndex, and
484 CollectAlignmentSummaryMetrics were used to sort, convert files, and generate alignment

485 metrics. The GATK (v4.1.2.0; Van der Auwera & O'Connor, 2020) HaplotypeCaller with default
486 parameters was used to call variants. GenomicsDBImport with default parameters was used to
487 merge the varieties into a single VCF file and genotyped using GenotypeGVCFs.Separated. SNPs
488 were selected using the SelectVariants command. Hard filtering of the SNPs was performed
489 using the parameters QD < 2.0, QUAL < 30.0, SOR > 3.0, FS > 60.0, MQ < 40.0, MQRankSum < -
490 12.5, MQRankSum-12.5, ReadPosRankSum < -8.0. Additional filtering was performed using
491 VCFTools (v0.1.16; Danecek et al., 2011) with filtering –freq2 and –max-alleles 2 to retain only
492 biallelic sites, minor allele frequency of 0.071, --max-missing 0.9, --minQ 30, --min-meanDP 15,
493 --max-meanDP 39.

494 SNPs were called relative to the Chia negra reference genome (Wang et al., 2022) using
495 nucmer from MUMmer (v4.0; Marçais et al., 2018) with the options –maxgap=2500, --
496 minmatch=11, and --mincluster=25. SNPs were quality filtered using the delta-filter command
497 in MUMmer with the -r flag. (v4.0; Marçais et al., 2018). The SNP set from the diversity panel
498 and from the alignment of the two genome assemblies were combined and converted into bed
499 format using PLINK 2.0 (v.alpha2.3; Purcell & Chang; Chang et al., 2015) resulting in 156,829
500 total SNPs. Population structure was inferred with Admixture (v.1.3.0; Alexander et al., 2009)
501 and a SNP phylogenetic tree built with SNPhylo (v.20160204; Lee et al., 2014) using default
502 parameters.

503 **ACKNOWLEDGMENTS**

504 Funds for this study were provided by a grant to C.R.B. from the National Science Foundation
505 Plant Genome Research Program (IOS-1444499), the Georgia Research Alliance, Georgia Seed
506 Development, and the University of Georgia. JB was supported by Michigan State University.

507 **CONTRIBUTIONS**

508 ACJ and CRB conceived of the study. SM-HGOR, PMM-P and ACP collected samples. PMM-P and
509 ACP prepared materials. JB, JPH, NS, DZ, JCW and BV performed data analyses and drafted the
510 manuscript. PPE, BH, ACJ, and CRB supervised and performed project administration. All
511 authors approved of the manuscript.

512

513 **DATA AVAILABILITY STATEMENT**

514 The raw sequence reads are available in the National Center for Biotechnology Information
515 Sequence Read Archive under BioProject PRJNA744892. The genome assembly, annotation, and
516 large data sets (genome assembly, genome annotation) reported in this study are available in
517 Figshare via 10.6084/m9.figshare.24546049.

518 **CONFLICT OF INTERESTS**

519 The authors declare no conflict of interests.

520

521 **REFERENCES**

522 Alejo-Jacuinde, G., Nájera-González, H.R., Chávez Montes, R.A., Gutierrez Reyes, C.D., Barragán-
523 Rosillo, A.C., Perez Sanchez, B., Mechref, Y., López-Arredondo, D., Yong-Villalobos, L., &
524 Herrera-Estrella, L. (2023). Multi-omic analyses reveal the unique properties of chia (*Salvia*
525 *hispanica*) seed metabolism. *Communications Biology*, 6. <https://doi.org/10.1038/s42003-023-05192-4>

527 Alexa, A., & Rahnenfuhrer, J. (2010). topGO: Enrichment Analysis for Gene Ontology

528 Alexander, D.H., Novembre, J., & Lange, K. (2009). Fast model-based estimation of ancestry in
529 unrelated individuals. *Genome Research*, 19, 1655–1664.
530 <https://doi.org/10.1101/gr.094052.109>

531 Van der Auwera, G.A., & O'Connor, B. (2020). *Genomics in the Cloud: Using Docker, GATK, and*
532 *WDL in Terra*. 1st Editio. O'Reilly Media.

533 Baldivia, A.S. (2018). A Historical Review of the Scientific and Common Nomenclature Associated
534 with Chia: From *Salvia hispanica* to *Salvia mexicana* and Chian to Salba. *Agricultural*
535 *Research & Technology: Open Access Journal*, 18.
536 <https://doi.org/10.19080/artoaj.2018.18.556047>

537 Bickhart, D.M., Rosen, B.D., Koren, S., Sayre, B.L., Hastie, A.R., Chan, S., Lee, J., Lam, E.T., Liachko,
538 I., Sullivan, S.T., Burton, J.N., Huson, H.J., Nystrom, J.C., Kelley, C.M., Hutchison, J.L., Zhou,
539 Y., Sun, J., Crisà, A., Ponce De León, F.A., Schwartz, J.C., Hammond, J.A., Waldbieser, G.C.,
540 Schroeder, S.G., Liu, G.E., Dunham, M.J., Shendure, J., Sonstegard, T.S., Phillippy, A.M., Van
541 Tassell, C.P., & Smith, T.P.L. (2017). Single-molecule sequencing and chromatin
542 conformation capture enable de novo reference assembly of the domestic goat genome.
543 *Nature Genetics*, 49, 643–650. <https://doi.org/10.1038/ng.3802>

544 Bornowski, N., Hamilton, J.P., Liao, P., Wood, J.C., Dudareva, N., & Buell, C.R. (2020). Genome
545 sequencing of four culinary herbs reveals terpenoid genes underlying chemodiversity in the
546 Nepetoideae. *DNA Research*, 27, 1–12. <https://doi.org/10.1093/dnare/dsaa016>

547 Bray, N.L., Pimentel, H., Melsted, P., & Pachter, L. (2016). Near-optimal probabilistic RNA-seq
548 quantification. *Nature Biotechnology*, 34, 525–527. <https://doi.org/10.1038/nbt.3519>

549 Brúna, T., Hoff, K.J., Lomsadze, A., Stanke, M., & Borodovsky, M. (2021). BRAKER2: Automatic
550 eukaryotic genome annotation with GeneMark-EP+ and AUGUSTUS supported by a protein
551 database. *NAR Genomics and Bioinformatics*, 3, 1–11.
552 <https://doi.org/10.1093/nargab/lqaa108>

553 Cahill, J.P. (2003). Ethnobotany of Chia, *Salvia hispanica* L. (Lamiaceae). *Economic Botany*, 57,
554 604–618. [https://doi.org/10.1663/0013-0001\(2003\)057\[0604:EOCSHL\]2.0.CO;2](https://doi.org/10.1663/0013-0001(2003)057[0604:EOCSHL]2.0.CO;2)

555 Cahill, J.P. (2004). Genetic diversity among varieties of Chia (*Salvia hispanica* L.). *Genetic
556 Resources and Crop Evolution*, 51, 773–781.
557 <https://doi.org/10.1023/B:GRES.0000034583.20407.80>

558 Campbell, M.A., Haas, B.J., Hamilton, J.P., Mount, S.M., & Robin, C.R. (2006). Comprehensive
559 analysis of alternative splicing in rice and comparative analyses with Arabidopsis. *BMC
560 Genomics*, 7, 1–17. <https://doi.org/10.1186/1471-2164-7-327>

561 Campbell, M.S., Law, M.Y., Holt, C., Stein, J.C., Moghe, G.D., Hufnagel, D.E., Lei, J.,
562 Achawanantakun, R., Jiao, D., Lawrence, C.J., Ware, D., Shiu, S.H., Childs, K.L., Sun, Y., Jiang,
563 N., & Yandell, M. (2014). MAKER-P: A Tool kit for the rapid creation, management, and
564 quality control of plant genome annotations. *Plant Physiology*, 164, 513–524.
565 <https://doi.org/10.1104/pp.113.230144>

566 Chang, C.C., Chow, C.C., Tellier, L.C.A.M., Vattikuti, S., Purcell, S.M., & Lee, J.J. (2015). Second-
567 generation PLINK: Rising to the challenge of larger and richer datasets. *GigaScience*, 4, 1–
568 16. <https://doi.org/10.1186/s13742-015-0047-8>

569 Danecek, P., Auton, A., Abecasis, G., Albers, C.A., Banks, E., DePristo, M.A., Handsaker, R.E.,
570 Lunter, G., Marth, G.T., Sherry, S.T., McVean, G., & Durbin, R. (2011). The variant call format
571 and VCFtools. *Bioinformatics*, 27, 2156–2158.
572 <https://doi.org/10.1093/bioinformatics/btr330>

573 Dong, A.X., Xin, H.B., Li, Z.J., Liu, H., Sun, Y.Q., Nie, S., Zhao, Z.N., Cui, R.F., Zhang, R.G., Yun, Q.Z.,
574 Wang, X.N., Maghly, F., Porth, I., Cong, R.C., & Mao, J.F. (2018). High-quality assembly of
575 the reference genome for scarlet sage, *Salvia splendens*, an economically important
576 ornamental plant. *GigaScience*, 7, 1–10. <https://doi.org/10.1093/gigascience/giy068>

577 Doyle, J.J., & Doyle, J.L. (1987). A rapid DNA isolation procedure from small quantities of fresh
578 leaf tissues.. *Pytochemical Bulletin*, 19, 11–15

579 Durand, N.C., Robinson, J.T., Shamim, M.S., Machol, I., Mesirov, J.P., Lander, E.S., & Aiden, E.L.
580 (2016). Juicebox Provides a Visualization System for Hi-C Contact Maps with Unlimited
581 Zoom. *Cell Systems*, 3, 99–101. <https://doi.org/10.1016/j.cels.2015.07.012>

582 Emms, D.M., & Kelly, S. (2019). OrthoFinder: Phylogenetic orthology inference for comparative
583 genomics. *Genome Biology*, 20, 238. <https://doi.org/10.1186/s13059-019-1832-y>

584 Fang, X., Li, C.Y., Yang, Y., Cui, M.Y., Chen, X.Y., & Yang, L. (2017). Identification of a novel (-)-5-
585 epieremophilene synthase from salvia miltiorrhiza via transcriptome mining. *Frontiers in*
586 *Plant Science*, 8, 1–11. <https://doi.org/10.3389/fpls.2017.00627>

587 Flynn, J.M., Hubley, R., Goubert, C., Rosen, J., Clark, A.G., Feschotte, C., & Smit, A.F. (2020).
588 RepeatModeler2 for automated genomic discovery of transposable element families.
589 *Proceedings of the National Academy of Sciences of the United States of America*, 117, 9451–
590 9457. <https://doi.org/10.1073/pnas.1921046117>

591 Godden, G.T., Kinser, T.J., Soltis, P.S., Soltis, D.E., & Chaw, S.M. (2019). Phylogenomic
592 Analyses Reveal Asymmetrical Gene Duplication Dynamics and Signatures of Ancient
593 Polyploidy in Mints. *Genome Biology and Evolution*, 11, 3393–3408.
594 <https://doi.org/10.1093/GBE/EVZ239>

595 Greene, D., Richardson, S., & Turro, E. (2017). OntologyX: A suite of R packages for working with
596 ontological data. *Bioinformatics*, 33, 1104–1106.
597 <https://doi.org/10.1093/bioinformatics/btw763>

598 Hamilton, J.P., Godden, G.T., Lanier, E., Bhat, W.W., Kinser, T.J., Vaillancourt, B., Wang, H., Wood,
599 J.C., Jiang, J., Soltis, P.S., Soltis, D.E., Hamberger, B., & Robin Buell, C. (2020). Generation of
600 a chromosome-scale genome assembly of the insect-repellent terpenoid-producing
601 Lamiaceae species, *Callicarpa americana*. *GigaScience*, 9, 1–11.
602 <https://doi.org/10.1093/gigascience/giaa093>

603 Hamilton, J.P., Vaillancourt, B., Wood, J.C., Wang, H., Jiang, J., Soltis, D.E., Buell, C.R., & Soltis, P.S.
604 (2023). Chromosome-scale genome assembly of the ‘Munstead’ cultivar of *Lavandula*
605 *angustifolia*. *BMC Genomic Data*, 24, 75

606 Han, M. V., Thomas, G.W.C., Lugo-Martinez, J., & Hahn, M.W. (2013). Estimating gene gain and
607 loss rates in the presence of error in genome assembly and annotation using CAFE 3.
608 *Molecular Biology and Evolution*, 30, 1987–1997. <https://doi.org/10.1093/molbev/mst100>

609 Hardigan, M.A., Crisovan, E., Hamilton, J.P., Kim, J., Laimbeer, P., Leisner, C.P., Manrique-
610 Carpintero, N.C., Newton, L., Pham, G.M., Vaillancourt, B., Yang, X., Zeng, Z., Douches, D.S.,
611 Jiang, J., Veilleux, R.E., & Buella, C.R. (2016). Genome reduction uncovers a large dispensable
612 genome and adaptive role for copy number variation in asexually propagated *Solanum*
613 *tuberosum*. *Plant Cell*, 28, 388–405. <https://doi.org/10.1105/tpc.15.00538>

614 He, Z., Feng, X., Chen, Q., Li, L., Li, S., Han, K., Guo, Z., Wang, J., Liu, M., Shi, C., Xu, S., Shao, S.,
615 Liu, X., Mao, X., Xie, W., Wang, X., Zhang, R., Li, G., Wu, W., Zheng, Z., Zhong, C., Duke, N.C.,
616 Boufford, D.E., Fan, G., Wu, C.I., Ricklefs, R.E., & Shi, S. (2022). Evolution of coastal forests
617 based on a full set of mangrove genomes. *Nature Ecology and Evolution*, 6, 738–749.
618 <https://doi.org/10.1038/s41559-022-01744-9>

619 Healey, A., Furtado, A., Cooper, T., & Henry, R.J. (2014). Protocol: A simple method for extracting
620 next-generation sequencing quality genomic DNA from recalcitrant plant species. *Plant
621 Methods*, 10, 1–8. <https://doi.org/10.1186/1746-4811-10-21/COMMENTS>

622 Hu, G.X., Takano, A., Drew, B.T., Liu, E. De, Soltis, D.E., Soltis, P.S., Peng, H., & Xiang, C.L. (2018).
623 Phylogeny and staminal evolution of *Salvia* (Lamiaceae, Nepetoideae) in East Asia. *Annals of
624 Botany*, 122, 649–668. <https://doi.org/10.1093/AOB/MCY104>

625 Jia, K.H., Liu, H., Zhang, R.G., Xu, J., Zhou, S.S., Jiao, S.Q., Yan, X.M., Tian, X.C., Shi, T. Le, Luo, H.,
626 Li, Z.C., Bao, Y.T., Nie, S., Guo, J.F., Porth, I., El-Kassaby, Y.A., Wang, X.R., Chen, C., Van de
627 Peer, Y., Zhao, W., & Mao, J.F. (2021). Chromosome-scale assembly and evolution of the
628 tetraploid *Salvia splendens* (Lamiaceae) genome. *Horticulture Research*, 8.
629 <https://doi.org/10.1038/s41438-021-00614-y>

630 Jones, P., Binns, D., Chang, H.-Y., Fraser, M., Li, W., McAnulla, C., McWilliam, H., Maslen, J.,
631 Mitchell, A., Nuka, G., Pesseat, S., Quinn, A.F., Sangrador-Vegas, A., Scheremetjew, M., Yong,
632 S.-Y., Lopez, R., & Hunter, S. (2014). InterProScan 5: genome-scale protein function
633 classification. *Bioinformatics*, 30, 1236–1240.
634 <https://doi.org/10.1093/bioinformatics/btu031>

635 Kautsar, S.A., Suarez Duran, H.G., Blin, K., Osbourn, A., & Medema, M.H. (2017). plantiSMASH:
636 automated identification, annotation and expression analysis of plant biosynthetic gene
637 clusters. *Nucleic Acids Research*, 45, W55–W63

638 Kim, D., Paggi, J.M., Park, C., Bennett, C., & Salzberg, S.L. (2019). Graph-based genome alignment
639 and genotyping with HISAT2 and HISAT-genotype. *Nature Biotechnology*, 37, 907–915.
640 <https://doi.org/10.1038/s41587-019-0201-4>

641 Koren, S., Walenz, B.P., Berlin, K., Miller, J.R., Bergman, N.H., & Phillippy, A.M. (2017). Canu:
642 Scalable and accurate long-read assembly via adaptive κ -mer weighting and repeat
643 separation. *Genome Research*, 27, 722–736. <https://doi.org/10.1101/gr.215087.116>

644 Kovaka, S., Zimin, A. V., Pertea, G.M., Razaghi, R., Salzberg, S.L., & Pertea, M. (2019).
645 Transcriptome assembly from long-read RNA-seq alignments with StringTie2. *Genome
646 Biology*, 20, 1–13. <https://doi.org/10.1186/s13059-019-1910-1>

647 Kumar, S., Suleski, M., Craig, J.M., Kasprowicz, A.E., Sanderford, M., Li, M., Stecher, G., & Hedges,
648 S.B. (2022). TimeTree 5: An Expanded Resource for Species Divergence Times. *Molecular*
649 *Biology and Evolution*, 39, 1–6. <https://doi.org/10.1093/molbev/msac174>

650 Lara-Cabrera, S.I., Perez-Garcia, M. de la L., Maya-Lastra, C.A., Montero-Castro, J.C., Godden,
651 G.T., Cibrian-Jaramillo, A., Fisher, A.E., & Porter, J.M. (2021). Phylogenomics of *Salvia* L.
652 subgenus *Calosphace* (Lamiaceae). *Frontiers in Plant Science*, 12.
653 <https://doi.org/10.3389/fpls.2021.725900>

654 Lee, T.H., Guo, H., Wang, X., Kim, C., & Paterson, A.H. (2014). SNPhylo: A pipeline to construct a
655 phylogenetic tree from huge SNP data. *BMC Genomics*, 15, 1–6.
656 <https://doi.org/10.1186/1471-2164-15-162>

657 Li, C.Y., Yang, L., Liu, Y., Xu, Z.G., Gao, J., Huang, Y.B., Xu, J.J., Fan, H., Kong, Y., Wei, Y.K., Hu, W.L.,
658 Wang, L.J., Zhao, Q., Hu, Y.H., Zhang, Y.J., Martin, C., & Chen, X.Y. (2022). The sage genome
659 provides insight into the evolutionary dynamics of diterpene biosynthesis gene cluster in
660 plants. *Cell Reports*, 40, 111236. <https://doi.org/10.1016/j.celrep.2022.111236>

661 Li, H. (2013). Aligning sequence reads, clone sequences and assembly contigs with BWA-MEM.
662 *arXiv preprint*, 1303.3997

663 Li, L., Song, J., Zhang, M., Iqbal, S., Li, Y., Zhang, H., & Zhang, H. (2023). A near complete genome
664 assembly of chia assists in identification of key fatty acid desaturases in developing seeds.
665 *Frontiers in Plant Science*, 14. <https://doi.org/10.3389/fpls.2023.1102715>

666 Lichman, B.R., Godden, G.T., Hamilton, J.P., Palmer, L., Kamileen, M.O., Zhao, D., Vaillancourt, B.,
667 Wood, J.C., Sun, M., Kinser, T.J., Henry, L.K., Rodriguez-Lopez, C., Dudareva, N., Soltis, D.E.,
668 Soltis, P.S., Robin Buell, C., & O'Connor, S.E. (2020). The evolutionary origins of the cat
669 attractant nepetalactone in catnip. *Science Advances*, 6, 1–14.
670 <https://doi.org/10.1126/sciadv.aba0721>

671 Lovell, J.T., Sreedasyam, A., Schranz, M.E., Wilson, M., Carlson, J.W., Harkess, A., Emms, D.,
672 Goodstein, D.M., & Schmutz, J. (2022). GENESPACE tracks regions of interest and gene copy
673 number variation across multiple genomes. *eLife*, 11, 1–20.
674 <https://doi.org/10.7554/ELIFE.78526>

675 Mapleson, D., Accinelli, G.G., Kettleborough, G., Wright, J., & Clavijo, B.J. (2017). KAT: A K-mer
676 analysis toolkit to quality control NGS datasets and genome assemblies. *Bioinformatics*, 33,
677 574–576. <https://doi.org/10.1093/bioinformatics/btw663>

678 Marçais, G., Delcher, A.L., Phillippy, A.M., Coston, R., Salzberg, S.L., & Zimin, A. (2018).
679 MUMmer4: A fast and versatile genome alignment system. *PLoS Computational Biology*, 14,
680 1–14. <https://doi.org/10.1371/journal.pcbi.1005944>

681 Marçais, G., & Kingsford, C. (2011). A fast, lock-free approach for efficient parallel counting of
682 occurrences of k-mers. *Bioinformatics*, 27, 764–770.
683 <https://doi.org/10.1093/bioinformatics/btr011>

684 Martin, M. (2011). Cutadapt removes adapter sequences from high-throughput sequencing
685 reads. *EMBnet.journal*, 17, 10–12

686 Mistry, J., Chuguransky, S., Williams, L., Qureshi, M., Salazar, G.A., Sonnhammer, E.L.L., Tosatto,
687 S.C.E., Paladin, L., Raj, S., Richardson, L.J., Finn, R.D., & Bateman, A. (2021). Pfam: The protein
688 families database in 2021. *Nucleic Acids Research*, 49, D412–D419.
689 <https://doi.org/10.1093/nar/gkaa913>

690 Mistry, J., Finn, R.D., Eddy, S.R., Bateman, A., & Punta, M. (2013). Challenges in homology search:
691 HMMER3 and convergent evolution of coiled-coil regions. *Nucleic Acids Res*, 41, e121.
692 <https://doi.org/10.1093/nar/gkt263>

693 Muñoz, L.A., Cobos, A., Diaz, O., & Aguilera, J.M. (2013). Chia Seed (*Salvia hispanica*): An Ancient
694 Grain and a New Functional Food. *Food Reviews International*, 29, 394–408.
695 <https://doi.org/10.1080/87559129.2013.818014>

696 Ou, S., Su, W., Liao, Y., Chougule, K., Agda, J.R.A., Hellinga, A.J., Lugo, C.S.B., Elliott, T.A., Ware,
697 D., Peterson, T., Jiang, N., Hirsch, C.N., & Hufford, M.B. (2019). Benchmarking transposable
698 element annotation methods for creation of a streamlined, comprehensive pipeline.
699 *Genome Biology*, 20, 1–18. <https://doi.org/10.1186/s13059-019-1905-y>

700 Pacfici Biosciences. SMRT tools.

701 Pan, X., Chang, Y., Li, C., Qiu, X., Cui, X., Meng, F., Zhang, S., Li, X., & Lu, S. (2023). Chromosome-
702 level genome assembly of *Salvia miltiorrhiza* with orange roots uncovers the role of
703 Sm2OGD3 in catalyzing 15,16-dehydrogenation of tanshinones. *Horticulture Research*, 10.
704 <https://doi.org/10.1093/hr/uhad069>

705 Peláez, P., Orona-Tamayo, D., Montes-Hernández, S., Valverde, M.E., Paredes-López, O., &
706 Cibrián-Jaramillo, A. (2019). Comparative transcriptome analysis of cultivated and wild
707 seeds of *Salvia hispanica* (chia). *Scientific Reports*, 9, 1–11. <https://doi.org/10.1038/s41598-019-45895-5>

709 Picard toolkit. (2019). *Broad Institute, GitHub repository*,

710 Purcell, S., & Chang, C. PLINK 2.0 alpha 2. 3

711 Ranallo-Benavidez, T.R., Jaron, K.S., & Schatz, M.C. (2020). GenomeScope 2.0 and Smudgeplot
712 for reference-free profiling of polyploid genomes. *Nature Communications*, 11.
713 <https://doi.org/10.1038/s41467-020-14998-3>

714 Roach, M.J., Schmidt, S.A., & Borneman, A.R. (2018). Purge Haplotts: allelic contig reassignment
715 for third-gen diploid genome assemblies.. *BMC bioinformatics*, 19, 460.
716 <https://doi.org/10.1186/s12859-018-2485-7>

717 Roberts, A., Trapnell, C., Donaghey, J., Rinn, J.L., & Pachter, L. (2011). Improving RNA-Seq
718 expression estimates by correcting for fragment bias. *Genome Biology*, 12.
719 <https://doi.org/10.1186/gb-2011-12-3-r22>

720 Shen, Y., Li, W., Zeng, Y., Li, Z., Chen, Y., Zhang, J., Zhao, H., Feng, L., Ma, D., Mo, X., Ouyang, P.,
721 Huang, L., Wang, Z., Jiao, Y., & Wang, H. bin. (2022). Chromosome-level and haplotype-
722 resolved genome provides insight into the tetraploid hybrid origin of patchouli. *Nature
723 Communications*, 13, 1–15. <https://doi.org/10.1038/s41467-022-31121-w>

724 Sievers, F., Wilm, A., Dineen, D., Gibson, T.J., Karplus, K., Li, W., Lopez, R., McWilliam, H.,
725 Remmert, M., Söding, J., Thompson, J.D., & Higgins, D.G. (2011). Fast, scalable generation of
726 high-quality protein multiple sequence alignments using Clustal Omega. *Molecular Systems
727 Biology*, 7. <https://doi.org/10.1038/msb.2011.75>

728 Simão, F.A., Waterhouse, R.M., Ioannidis, P., Kriventseva, E. V., & Zdobnov, E.M. (2015). BUSCO:
729 assessing genome assembly and annotation completeness with single-copy orthologs.
730 *Bioinformatics*, 31, 3210–3212. <https://doi.org/10.1093/bioinformatics/btv351>

731 Smit, A., Hubley, R., & Green, P. *RepeatMasker Open-4.0*.

732 Stamatakis, A. (2014). RAxML version 8: a tool for phylogenetic analysis and post-analysis of large
733 phylogenies. *Bioinformatics*, 30, 1312–1313.
734 <https://doi.org/10.1093/bioinformatics/btu033>

735 Sun, M., Zhang, Y., Zhu, L., Liu, N., Bai, H., Sun, G., Zhang, J., & Shi, L. (2022). Chromosome-level
736 assembly and analysis of the *Thymus* genome provide insights into glandular secretory
737 trichome formation and monoterpenoid biosynthesis in thyme. *Plant Communications*, 3,
738 100413. <https://doi.org/10.1016/j.xplc.2022.100413>

739 Tamura, K., Sakamoto, M., Tanizawa, Y., Mochizuki, T., & Bono, H. (2022). Resource Article :
740 Genomes Explored A highly contiguous genome assembly of red perilla (*Perilla frutescens*)
741 domesticated in Japan 1–8

742 Valdivia-López, M.Á., & Tecante, A. (2015). Chia (*Salvia hispanica*): A Review of Native Mexican
743 Seed and its Nutritional and Functional Properties. *Advances in Food and Nutrition Research*
744 (pp. 53–75). Academic Press Inc.

745 Walker, B.J., Abeel, T., Shea, T., Priest, M., Abouelliel, A., Sakthikumar, S., Cuomo, C.A., Zeng, Q.,
746 Wortman, J., Young, S.K., & Earl, A.M. (2014). Pilon: An Integrated Tool for Comprehensive
747 Microbial Variant Detection and Genome Assembly Improvement. *PLoS ONE*, 9, e112963.
748 <https://doi.org/10.1371/journal.pone.0112963>

749 Wang, L., Lee, M., Sun, F., Song, Z., Yang, Z., & Yue, G.H. (2022). A chromosome-level genome
750 assembly of chia provides insights into high omega-3 content and coat color variation of its
751 seeds. *Plant Communications*, 3, 100326. <https://doi.org/10.1016/j.xplc.2022.100326>

752 Wang, Y., Tang, H., Debarry, J.D., Tan, X., Li, J., Wang, X., Lee, T.H., Jin, H., Marler, B., Guo, H.,
753 Kissinger, J.C., & Paterson, A.H. (2012). MCScanX: a toolkit for detection and evolutionary
754 analysis of gene synteny and collinearity. *Nucleic Acids Res*, 40, e49.
755 <https://doi.org/10.1093/nar/gkr1293>

756 Xu, Z., Gao, R., Pu, X., Xu, R., Wang, J., Zheng, S., Zeng, Y., Chen, J., He, C., & Song, J. (2020).
757 Comparative Genome Analysis of *Scutellaria baicalensis* and *Scutellaria barbata* Reveals the
758 Evolution of Active Flavonoid Biosynthesis. *Genomics, Proteomics and Bioinformatics*, 18,
759 230–240. <https://doi.org/10.1016/j.gpb.2020.06.002>

760 Zhang, Y., Shen, Q., Leng, L., Zhang, D., Chen, S., Shi, Y., Ning, Z., & Chen, S. (2021). Incipient
761 diploidization of the medicinal plant Perilla within 10,000 years. *Nature Communications*,
762 12, 1–13. <https://doi.org/10.1038/s41467-021-25681-6>

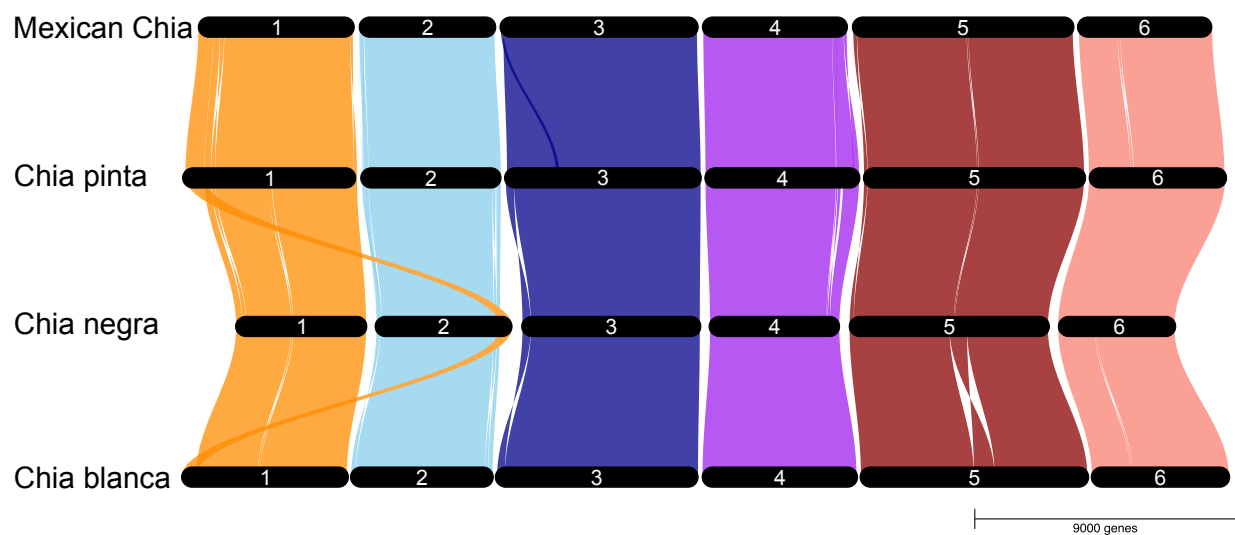
763 Zhao, D., Hamilton, J., Bhat, W., Johnson, S., Godden, G., Kinser, T., Boachon, B., Dudareva, D.,
764 Soltis, P., & Soltis, D. (2019)(a). A chromosomal-scale genome assembly of *Tectona grandis*
765 reveals the importance of tandem gene duplication and enables discovery of genes in
766 natural product biosynthetic pathways. *GigaScience*, 8, giz005

767 Zhao, Q., Yang, J., Cui, M.Y., Liu, J., Fang, Y., Yan, M., Qiu, W., Shang, H., Xu, Z., Yidireshi, R., Weng,
768 J.K., Pluskal, T., Vigouroux, M., Steuernagel, B., Wei, Y., Yang, L., Hu, Y., Chen, X.Y., & Martin,
769 C. (2019)(b). The Reference Genome Sequence of *Scutellaria baicalensis* Provides Insights
770 into the Evolution of Wogonin Biosynthesis. *Molecular Plant*, 12, 935–950.
771 <https://doi.org/10.1016/j.molp.2019.04.002>

772

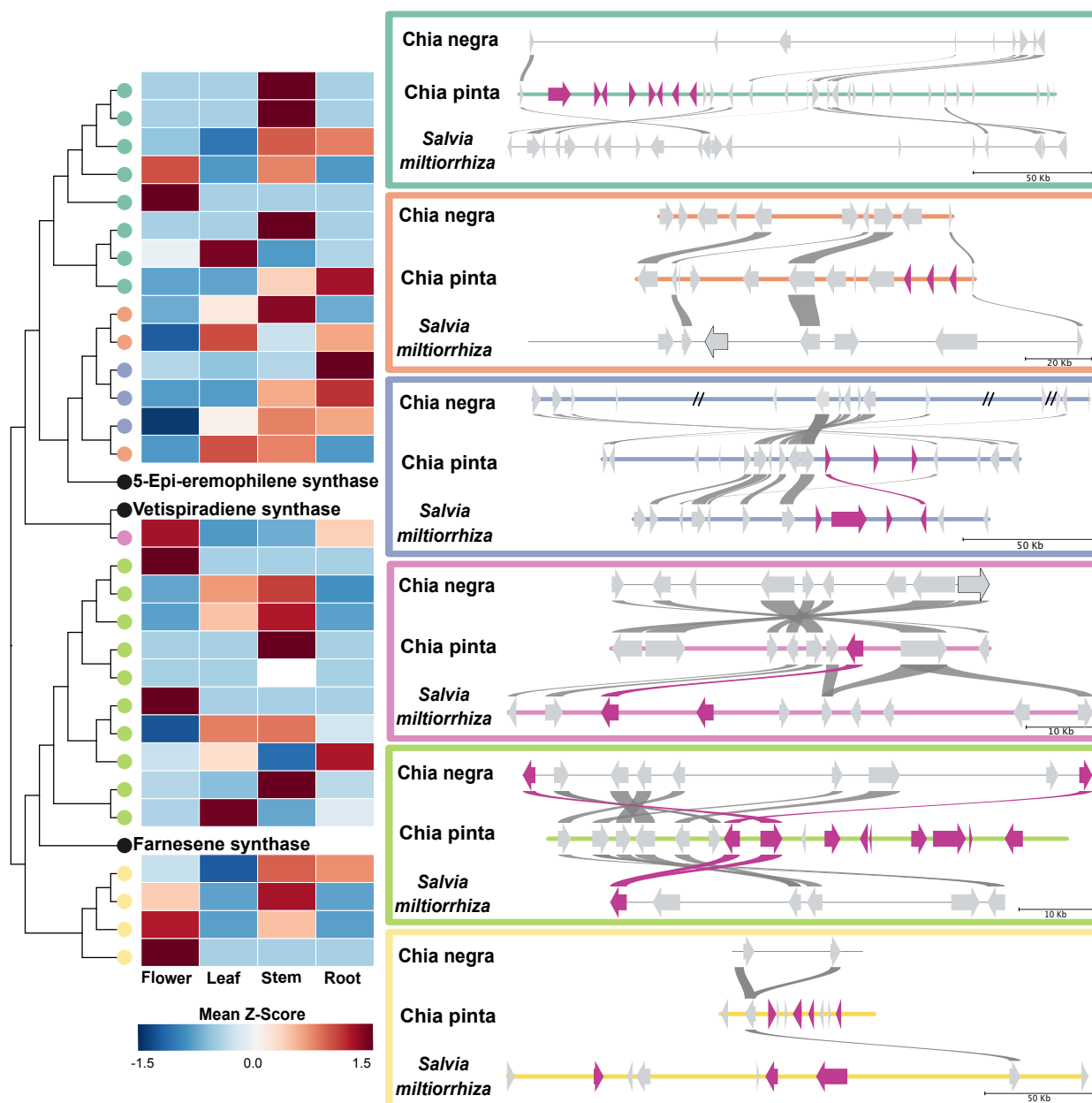
773

774 **Figures and Tables**



775

776 **Figure 1. Synteny of the Chia genomes.** The top track is the Mexican Chia genome (Alejo-
777 Jacuinde et al., 2023), the second track is the Chia pinta genome reported in this study, the
778 third genome is Chia negra (Wang et al., 2022), and the bottom track represents the Chia
779 blanca genome (Li et al., 2023). The ribbons indicate syntenic blocks between the genomes
780 identified using GENESPACE (v.1.1.10; Lovell et al., 2022).

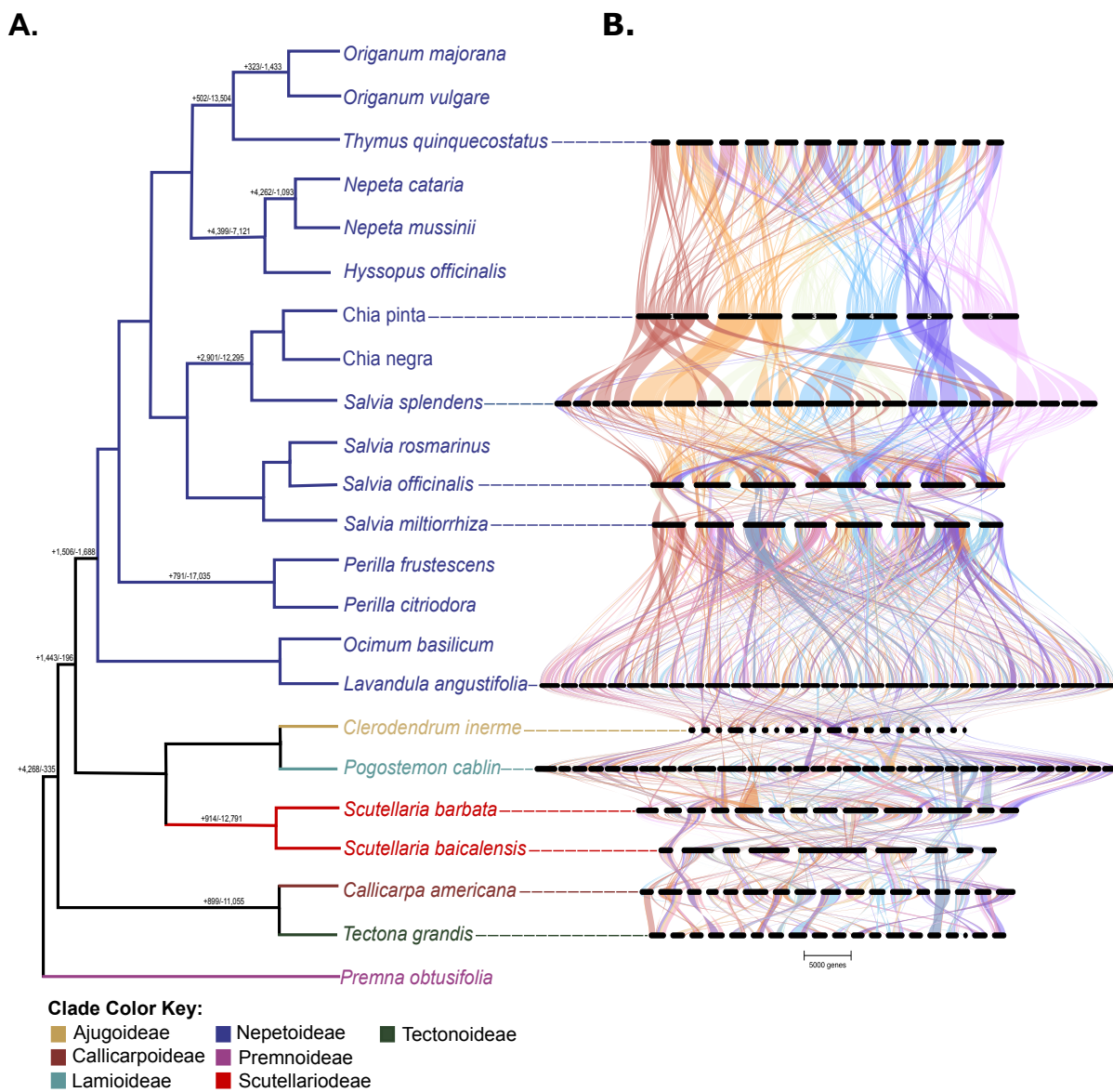


781

782 **Figure 2. Chia pinta TPS-a Biosynthetic Gene Cluster Expression and Synteny.** A phylogeny of
783 the Chia pinta terpene synthase (TPS-a) genes present in biosynthetic gene clusters (BGCs) with
784 representative functionally characterized reference TPSs is shown. The Chia pinta phylogeny
785 was generated using RAxML (v8.2.12; Stamatakis, 2014). The heatmap of gene expression was
786 constructed from flower, leaf, stem, and root tissue using expression values generated by
787 Cufflinks (v.2.2.1; Roberts et al., 2011) with z-scores range from -1.5 to 1.5. Chia pinta genes
788 (circles on the phylogeny) are colored by their respective BGC and correspond to the outlined
789 syntenic BGCs; genes in black are known TPS. Biosynthetic gene clusters (BGCs) were identified
790 by PlantSmash (Kautsar et al., 2017) with boxes colored to match the clades in the phylogeny.
791 Syntenic regions were determined using MCSpanX (Wang et al., 2012) between Chia pinta, Chia

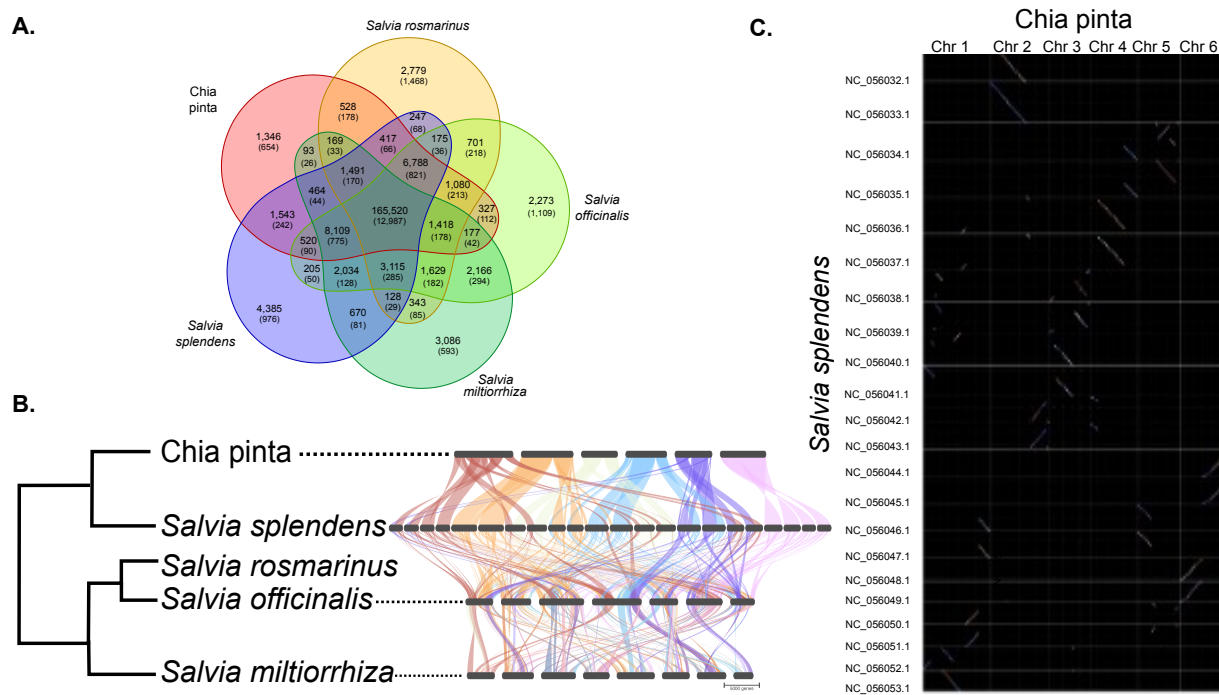
792 negra, and *S. miltorrhiza*. Synteny is indicated as lines between the genes (arrows). The color of
793 the gene and syntetic line is determined by the presumed identity assigned by PlantSmash
794 where hot pink indicate TPSs; slashes through the line indicate gaps in the assembly. Grey
795 genome lines indicate that it is not a TPS BGC.

796



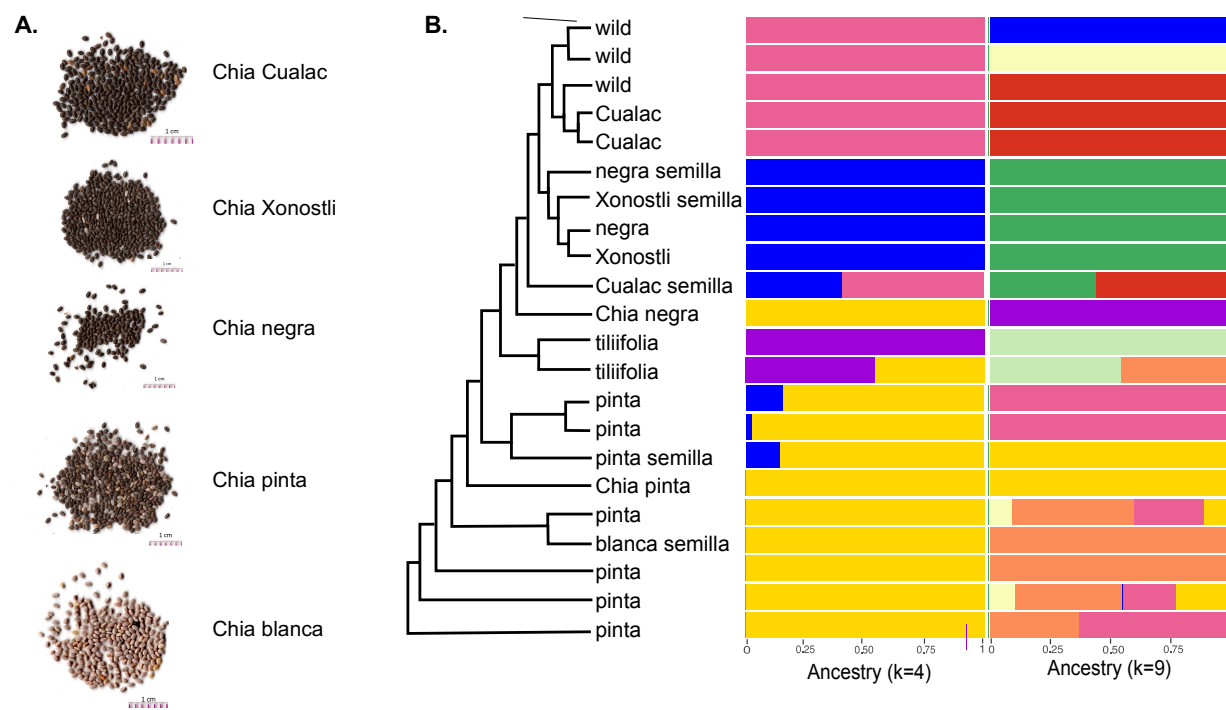
797

798 **Figure 3. Lamiaceae phylogeny and synteny.** **A.** A species phylogeny was generated using
799 OrthoFinder (v.2.5.4; Emms & Kelly, 2019) using publicly available chromosome-scale Lamiaceae
800 genomes. Numbers on branches indicated with (+) are gene family expansions and (-) are gene
801 family contractions using CAFE (v.4.2.1; Han et al., 2013). **B.** The GENESPACE (v.1.1.10; Lovell et
802 al., 2022) synteny map of orthologous regions within chromosome-scale Lamiaceae genome
803 assemblies are shown using the Chia pinta as the reference genome. Chromosomes are scaled
804 by their physical length.



805

806 **Figure 4. *Salvia* gene orthology and synteny. A.** *Salvia* orthogroup intersections between Chia
807 pinta, *Salvia rosmarinus*, *Salvia officinalis*, *Salvia splendens*, and *Salvia miltiorrhiza* as
808 determined by OrthoFinder (v.2.5.4; Emms & Kelly, 2019). Numbers of orthologous groups and
809 genes in parentheses are reported. **B.** GENESPACE (v.1.1.10; Lovell et al., 2022) synteny map of
810 orthologous regions within chromosome-scale *Salvia* genome assemblies using Chia pinta as
811 the reference genome. **C.** Synteny dotplot for the anchor genes between Chia pinta and *Salvia*
812 *splendens* generated in GENESPACE (v.1.1.10; Lovell et al., 2022). Chia pinta includes 21,720
813 genes with BLAST hits. *Salvia splendens* includes 25,958 genes with blast hits.



814

815 **Figure 5. Population structure of Chia.** **A.** Representative seed images of Chia varieties. **B.** SNP
816 phylogeny was built using SNPhylo (v.20160204; Lee et al., 2014). Admixture (v.1.3.0; Alexander
817 et al., 2009) population structure of 20 Chia accessions and 2 *Salvia tiliifolia* accessions was
818 generated from 156,829 SNPs. Populations from the minima on the cross-validation plot was
819 determined using $k=4$ and $k=9$.

820

821

822

823

824

Table 1. Chia pinta Genome Assembly Metrics

	Input assembly	Purged Assembly	Final Chromosome-scale Assembly
Number of Contigs/	2,094	407	6
Chromosomes			
Total length (bp)	425,143,449	343,219,856	341,980,016
Maximum Contig Length (bp)	9,374,111	9,374,111	67,233,260
Minimum Contig Length (bp)	1,684	2,780	57,181,130
N50 Contig Length (bp)	1,150,825	1,506,829	62,351,092
Average Contig Length (bp)	203,029	858,050	56,996,669

825

826

Table 2. Chia pinta Genome Annotation Metrics

	High Confidence Model Set	High Confidence Representative Model Set	Working Model Set	Working Model Representative Set
Number of Gene Models	53,053	35,480	59,062	41,279
Number of Loci	35,480	35,480	41,279	41,279
Average Transcript Length (bp)	3,300.5	2,889.0	3,104.3	2,661.1
Average CDS Length (bp)	1,283.4	1,196.6	1,216.8	1,109.9
Average Exon Length (bp)	280.2	283.7	279.1	280.8
Average Intron Length (bp)	244.2	229.8	239.8	225.2
Average No. Exons per Model	6.1	5.3	5.8	4.9
Single Exon Transcripts	6,105	6,043	8,062	7,999

827